Cyclic Contact Fatigue of Brittle Ceramics

B.R. Lawn, D.K. Kim, S.K. Lee, Y-G. Jung and I.M. Peterson

The Seventh International Fatigue Conference

Fatigue 99

Beijing, China, Vol. 1, p. 69, 1999

CYCLIC CONTACT FATIGUE OF BRITTLE CERAMICS

Brian Lawn, Do Kyung Kim, Seung-Kun Lee, Yeon-Gil Jung, Irene M. Peterson

Materials Science and Engineering Laboratory
National Institute of Standards and Technology
Gaithersburg, MD 20899

Contact damage modes in cyclic loading with spheres are investigated in several ceramics, principally silicon nitride but also some ceramics used for dental restorations. Initial damage at small numbers of cycles and low loads consists of tensile-driven macroscopic cone cracks ("brittle" mode). Secondary damage at large numbers of cycles and high loads consists of shear-driven distributed microdamage ("quasi-plastic" mode), with attendant radial cracks. Strength tests on indented specimens are used to quantify the degree of damage. Both damage modes degrade the strength: the first, immediately after cone crack initiation, relatively slowly; the second, after development of radial cracks, much more rapidly. Comparison with static contact data indicates a strong mechanical (as opposed to chemical) component in the cyclic fatigue in the quasi-plastic region. The basis for setting up fracture mechanics models is briefly discussed.

1. INTRODUCTION

Many studies have shown that increasing microstructural heterogeneity (e.g. by coarsening and elongating grains, and introducing weak boundaries) toughens ceramics in the long-crack region, primarily by enhancing bridging (1-4). It also makes these same ceramics susceptible to fatigue in cyclic loading, by degrading the bridging (5,6)—enhanced toughness and improved fatigue resistance tend to be mutually exclusive. This inverse relation between fatigue susceptibility and toughness extends to the strongest ceramics, including silicon nitride (7-10).

Fatigue susceptibility of tough ceramics is even more dramatic in Hertzian contacts (11-13). A schematic of the Hertzian contact fatigue test is shown in Fig. 1. Fundamentally different damage modes are observed, depending on the ceramic microstructure: in homogeneous, fine-grain microstructures, conical cracks form at the specimen surface around the contact circle ("Hertzian cone" fractures), where limited tension occurs ("brittle" mode) (14); in heterogeneous, coarse-grain microstructures, distributed microslip events develop within a subsurface zone below the contact, driven by shear stresses ("quasi-plastic" mode) (15).

In the present paper we investigate the influence of microstructure on Hertzian contact fatigue in silicon nitride used in bearing applications (16,17); and in some other, less strong ceramics designed for dental restorations (18,19). In both bearing and dental applications contact stresses are critical in the materials function. The questions arise—how does the microstructure affect the fatigue and strength after *repeated* contacts, and what are the contact fatigue properties? We briefly address these questions here.

2. SILICON NITRIDE

The silicon nitride materials used here are described in detail elsewhere (16,20): (i) "fine" (F-Si_3N_4), a bimodal microstructure with mainly small equiaxed α grains (< 1 μm) and some elongated β grains; (ii) "medium" (M-Si_3N_4), a bimodal microstructure with a larger fraction of elongated β grains of (length $\approx$4 μm); (iii) "coarse" (C-Si_3N_4), a microstructure with predominantly elongated β grains (length $\approx$9 μm). Each material contains $\approx$ 10 vol% interboundary glassy phase. These materials have increasing toughness in the sequence FMC.

The nature of single-cycle contact damage in these silicon nitrides using tungsten carbide (WC) spheres is revealed in Fig. 1 (16), showing top-surface and side-section views of typical damage patterns: (a) F-Si_3N_4, large cone cracks, no detectable quasi-plasticity; (b) M-Si_3N_4, smaller but still well-developed cone cracks, small quasi-plasticity below the contact; (c) C-Si_3N_4, vestigial surface ring cracks, dominant quasi-plasticity.

The severity of contact damage is most easily quantified by conducting fast-fracture strength tests on indented flexure bars, with the damaged region centered on the tensile face. Results of such tests on the silicon nitrides are shown in Fig. 3, as a function of number of cycles n at specified maximum contact load P, tests in air. In Fig. 3a, the indentation load P = 1000 N is much lower than that required to initiate damage in a single cycle. After $\approx 10^4$–10^5 cycles the strength falls off, abruptly in the F-Si_3N_4 and M-Si_3N_4 due to initiation of cone cracks, and more gradually in the C-Si_3N_4 from progressive accumulation of quasi-plastic damage. In Fig. 3b, at P = 2200 N, strength degrading damage is incurred after a single cycle, and strength falls off progressively thereafter. Note at both loads that the strength degradation is initially least in the C-Si_3N_4, but accelerates much more rapidly in this same material at large n. Whereas the degradation in the F and M material can be accounted for by conventional slow growth of cone cracks, in the tougher C material the degradation involves coalescence of microcracks within the damage zone (21).

Figure 4 compares strength data for cyclic and static contacts in F-Si_3N_4, M-Si_3N_4 and C-Si_3N_4, at P = 2200 N. The results are plotted as a function of contact time (upper axis) as well as number of cycles (lower axis), to facilitate direct intercomparisons. In the F and M materials the static data sets are barely distinguishable from the cyclic data sets over most of the data range (i.e. except perhaps at $n = 10^7$ in M-Si_3N_4). In the C material, on the other hand, the cyclic data set falls significantly lower than the static data set, the more so at high n. There is a clear mechanical component in the quasi-plastic fatigue process in the tougher materials.

3. OTHER CERAMICS

Similar fatigue testing studies have been carried out on several ceramics used for dental restorations, especially crowns (18,19). These studies are useful for the range of microstructures and strength values covered, and so highlight the generality of the contact fatigue phenomenon in ceramics. Materials include porcelain and micaceous glass-ceramics used for dental veneers, chosen not for their strength but for their aesthetics. Other materials include glass-infiltrated aluminas and zirconia (Y-TZP) for underlying support for the veneer, chosen for their toughness.

Figure 5 is a plot of strength as a function of number of contact cycles for a dental porcelain. Note that the strengths are much lower than the silicon nitride. Data are shown for two loads. At P = 200 N, the damage is on the threshold for cone cracking in the contact test. Consequently, strengths are bimodal, and are slightly degraded or not degraded at all, depending on whether or not cracks form. At P = 500 N, the strengths are much more degraded, even after a single cycle. In this case the falloff is initially slow, as the cone cracks continue to extend during the cycling, but then fall off much more rapidly, as quasi-plastic damage builds up and ultimately dominates. There is a brittle–to–plastic transition in the damage process. After $\approx 10^5$ cycles the specimens actually fail during the contact testing.

Included in Fig. 5 are micrographs showing failure sites in the flexure tests, corresponding to points marked A, B, C in the strength plot (19). In A, the damage is classical ring crack, and the

failure initiates at the base of the cone crack outside the contact circle. In B, damage is seen accumulating within the original cone trace, and the failure now intersects the contact circle. In C, the damage has accumulated to the extent that material has spalled from the top surface. The process at high *n* is clearly one of microcrack coalescence within the contact zone.

Figure 6 shows closer views of the surface damage in each material studied, after sufficient contact to develop dominant quasi-plasticity (19). In each material except the Y-TZP, the specimen has been thinned from the rear surface opposite the indentation to allow viewing in transmitted light. These views show the presence of radial cracks emanating outward from the contact zone. (Faint traces are seen also in the Y-TZP, observed in reflected light.) *In situ* observations of such indentation sites during actual strength testing shows that the radial cracks are primary sources of failure, explaining the appearance of the fracture paths in B and C in Fig. 5.

4. DISCUSSION

Figure 7 is a "master diagram", combining strength degradation data for several ceramics, including very brittle glass, for contacts at specified loads. It is clear that all materials, even the toughest, are susceptible to fatigue. For reference, loads of 1000 N are typical of bearing stresses, and loads of 200–500 N occur in biting function in dental configurations. It is clear that it contact degradation can be an important factor in the design of ceramics for applications involving concentrated fields.

These results show how ceramic materials are subject to fatigue in repeat contact loading. In more brittle, homogeneous ceramics, conventional tensile-driven cone cracks provide the main source of initial degradation. At first pop-in, these cone cracks abruptly degrade the remaining strength. In continued cycling the cone cracks continue to extend, but slowly and stably, most strongly from chemical interaction with environmental water. In tougher, more heterogeneous ceramics, the mode is one of shear-driven microdamage beneath the indenter. Degradation from this mode is relatively gradual, but accelerates rapidly and ultimately dominates as microcracks coalescence, forming more deleterious radial cracks. This second mode is characterized by a strong mechanical component.

Theoretical models of the damage modes and their relation to strength are being developed. For the cone crack mode, linear elastic fracture mechanics can be used to specify stress intensity factors. In combination with time integration of an appropriate crack velocity function over the cyclic contact duration, these stress intensity factors can be used to map out the lifetime characteristics of brittle ceramics (22). For the quasi-plastic mode, the mechanics is more complex, involving detailed mechanics of individual, localized shear microcracks within the microstructure, along with some coalescence condition (21). Work on such models is continuing.

ACKNOWLEDGEMENTS

This work was funded in part by the National Institute for Standards and Technology (NIST internal funds) and in part by grants from the National Institutes for Dental Research (NIDR PO1 DE10976) and the Korea Science and Engineering Foundation (KOSEF).

REFERENCES

1 P. L. Swanson, C. J. Fairbanks, B. R. Lawn, Y.-W. Mai and B. J. Hockey, *Journal of the American Ceramic Society*, *70* (1987) 279-89.
2 S. J. Bennison and B. R. Lawn, *Acta Metallurgica*, *37* (1989) 2659-71.
3 S. J. Bennison and B. R. Lawn, *Journal of Materials Science*, *24* (1989) 3169-75.
4 S. J. Bennison, N. P. Padture, J. L. Runyan and B. R. Lawn, *Philosophical Magazine Letters*, *64* (1991) 191-95.

5 S. Lathabai, Y.-W. Mai and B. R. Lawn, *Journal of the American Ceramic Society*, *72* (1989) 1760-63.
6 S. Lathabai, J. Rödel and B. R. Lawn, *Journal of the American Ceramic Society*, *74* (1991) 1340-48.
7 R. H. Dauskardt, *Acta Metallurgica et Materialia*, *41* (1993) 2765-81.
8 D. S. Jacobs and I.-W. Chen, *Journal of the American Ceramic Society*, *77* (1994) 1153-61.
9 C. J. Gilbert, R. H. Dauskardt and R. O. Ritchie, *Journal of the American Ceramic Society*, *78* (1995) 2291-300.
10 R. O. Ritchie, *International Journal of Fracture*, (1998)
11 F. Guiberteau, N. P. Padture, H. Cai and B. R. Lawn, *Philosophical Magazine*, *A 68* (1993) 1003-16.
12 H. Cai, M. A. S. Kalceff, B. M. Hooks, B. R. Lawn and K. Chyung, *Journal of Materials Research*, *9* (1994) 2654-61.
13 N. P. Padture and B. R. Lawn, *Journal of the American Ceramic Society*, *78* (1995) 1431-38.
14 B. R. Lawn, *Fracture of Brittle Solids*, Cambridge University Press, Cambridge, 1993.
15 B. R. Lawn, N. P. Padture, H. Cai and F. Guiberteau, *Science*, *263* (1994) 1114-16.
16 S. K. Lee, S. Wuttiphan and B. R. Lawn, *Journal of the American Ceramic Society*, *80* (1997) 2367-81.
17 S. K. Lee and B. R. Lawn, *Journal of the American Ceramic Society*, *81* (1998) 997-1003.
18 I. M. Peterson, A. Pajares, B. R. Lawn, V. P. Thompson and E. D. Rekow, *Journal of Dental Research*, *77* (1998) 589-602.
19 Y.-G. Jung, I. M. Peterson, D. K. Kim and B. R. Lawn, *Journal of Dental Research*, (in preparation)
20 S. K. Lee and B. R. Lawn, *Journal of the American Ceramic Society*, (in press)
21 B. R. Lawn, S. K. Lee, I. M. Peterson and S. Wuttiphan, *Journal of the American Ceramic Society*, *81* (1998) 1509-20.
22 D. K. Kim, Y.-G. Jung, I. M. Peterson and B. R. Lawn, *Acta Materialia*, (in preparation)

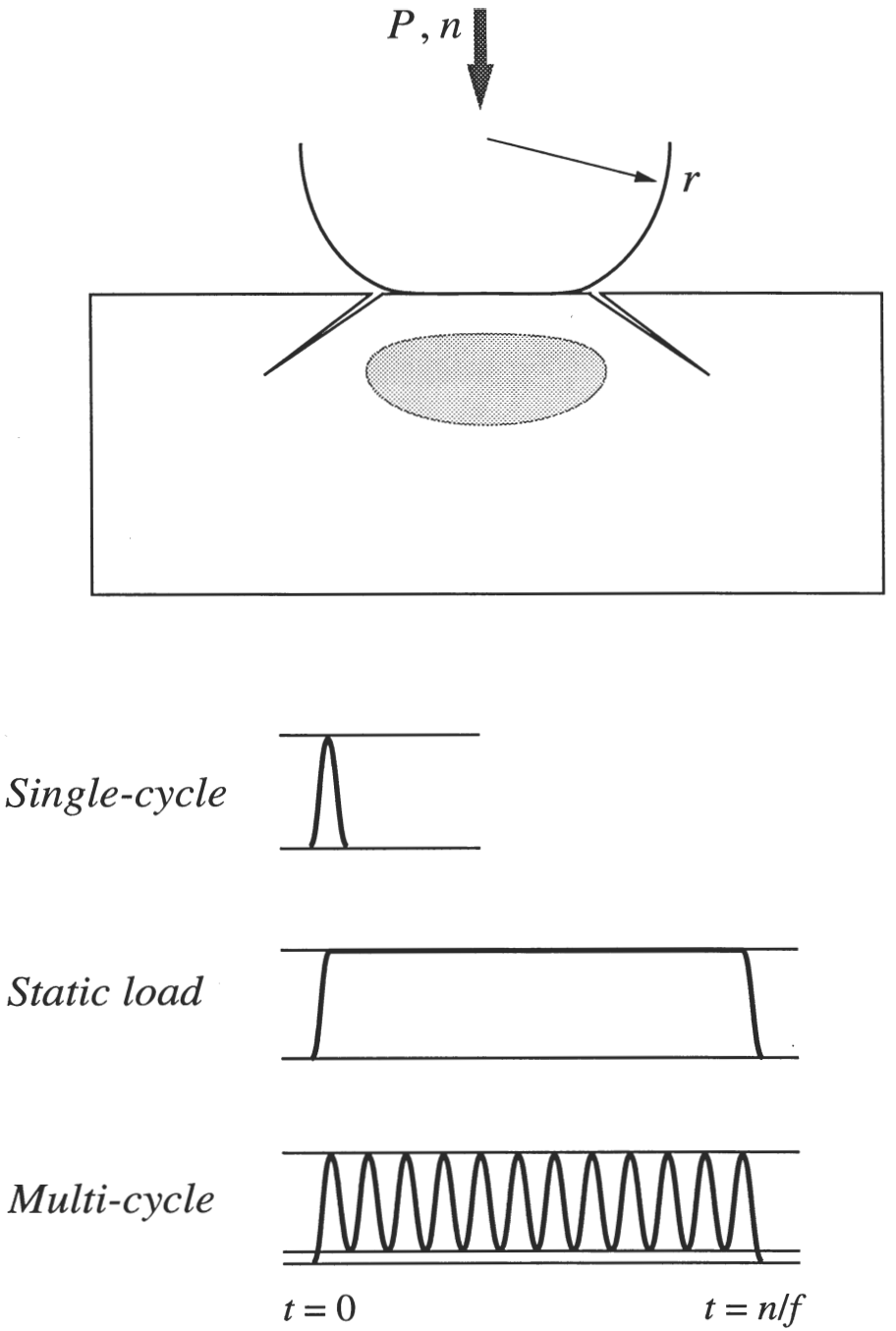

Fig. 1 Schematic of Hertzian contact test, with WC sphere of radius r and n cycles at load P. Beyond threshold load, damage consists of cone cracks; plus, under severe loading conditions, subsurface quasi-plastic deformation zone. Cyclic fatigue tests are run over n normal contacts at frequency f. Comparative single-cycle tests, and static loading tests over prescribed hold times t, are also run.

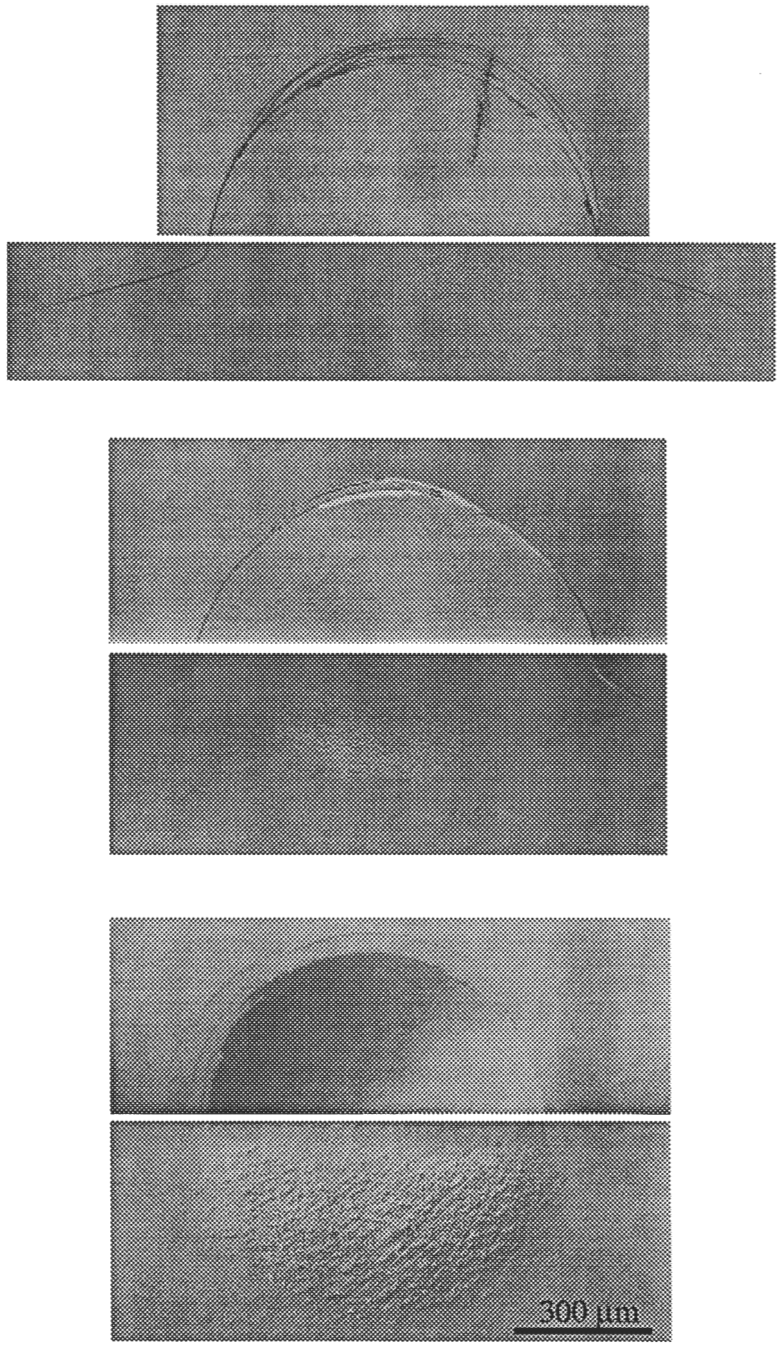

Fig. 2 Half-surface and side views of single-cycle Hertzian contact damage in (a) F-Si_3N_4, (b) M-Si_3N_4, (c) C-Si_3N_4, with WC spheres, r = 1.98 mm, in air, at load P = 4000 N. Nomarksi optical micrographs of bonded-interface specimen. Reproduced from (16).

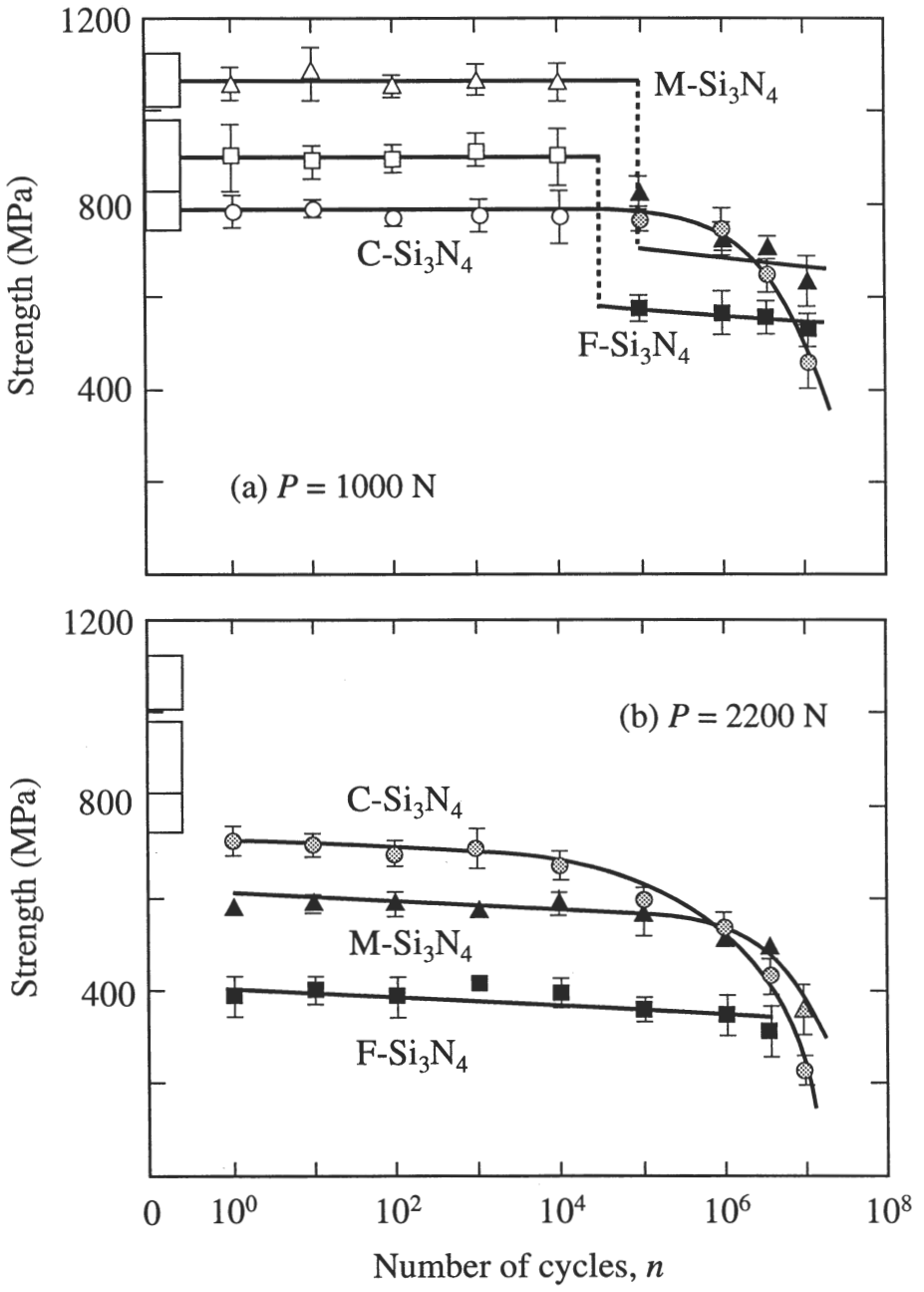

Fig 3. Strength as a function of number of contact cycles F-Si_3N_4, M-Si_3N_4, C-Si_3N_4, demonstrating role of microstructure. Indentation with WC spheres, r = 1.98 mm, in air, at loads P indicated. Black symbols indicate failure from cone cracks, grey symbols from quasi-plastic zones, open symbols from natural flaws. Boxes at left axis indicate "laboratory" strengths (unindented specimens).

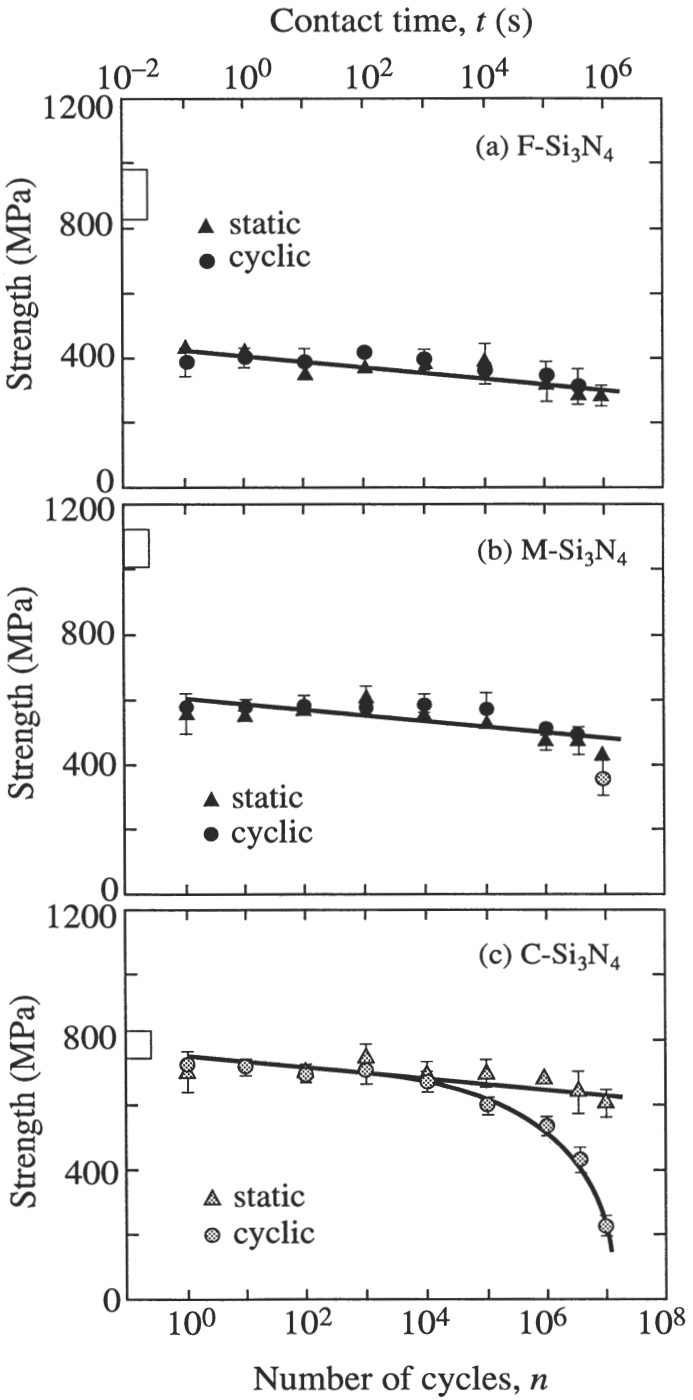

Fig. 4 Strength as a function of contact time for (a) F-Si_3N_4, (b) M-Si_3N_4, (c) C-Si_3N_4, comparing damage accumulation at static and cyclic contacts. Indentation with WC spheres, r = 1.98 mm, P = 2200 N, in air. Black symbols indicate failure from cone cracks, grey symbols from quasi plastic zones. Boxes at left axis indicate "laboratory"strengths.

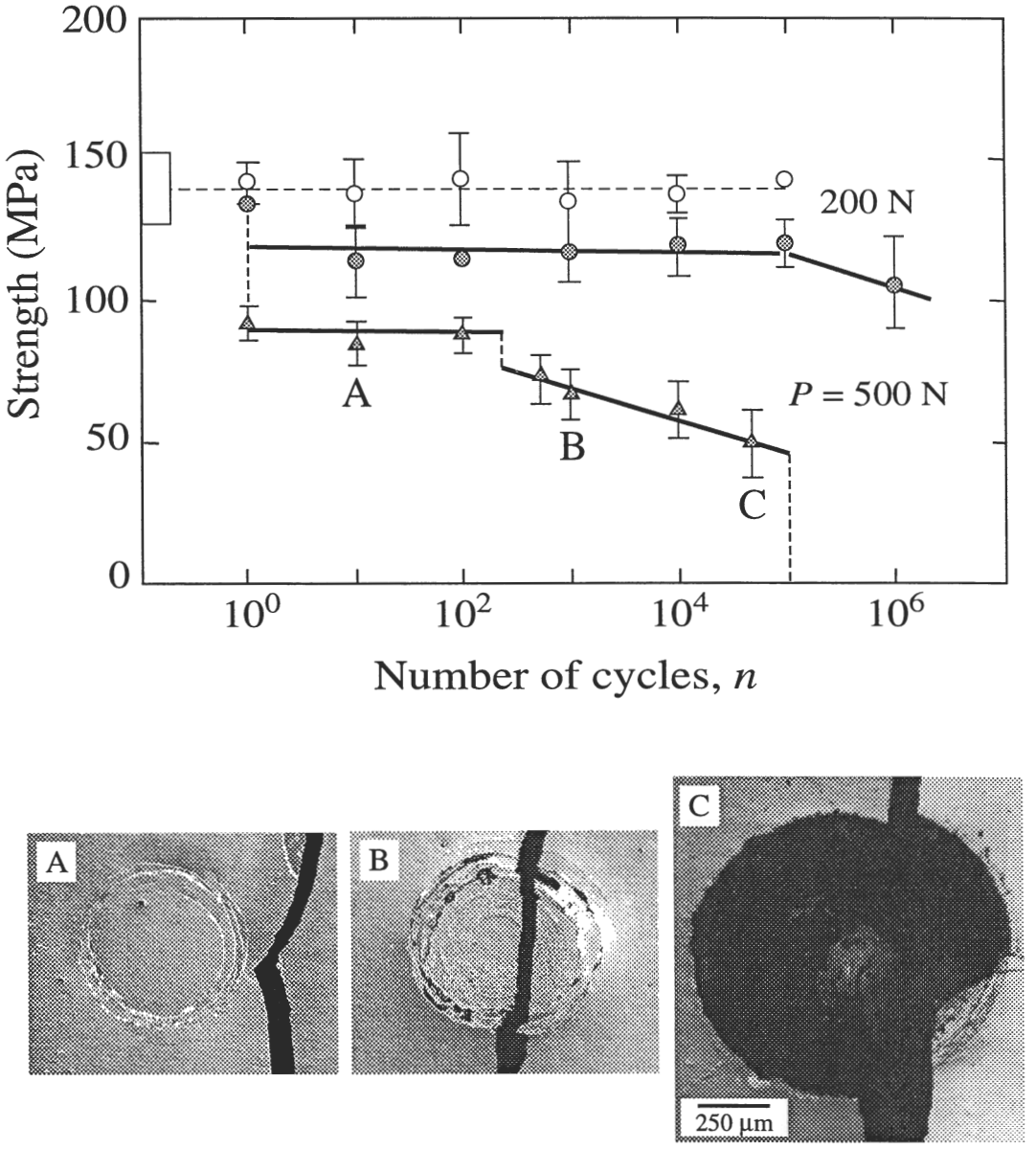

Fig. 5 Inert strength as a function of number of contact cycles n for porcelain. Indentation with WC spheres (r = 3.18 mm) at maximum loads P indicated, in water. Unfilled symbols indicate failures from natural flaws, filled symbols failures from indentation sites. Box at left axis indicates "laboratory" strengths . Reflected light micrographs (Nomarski illumination) show surface failure sites at points A, B and C marked on plot (flexural tension axis horizontal).

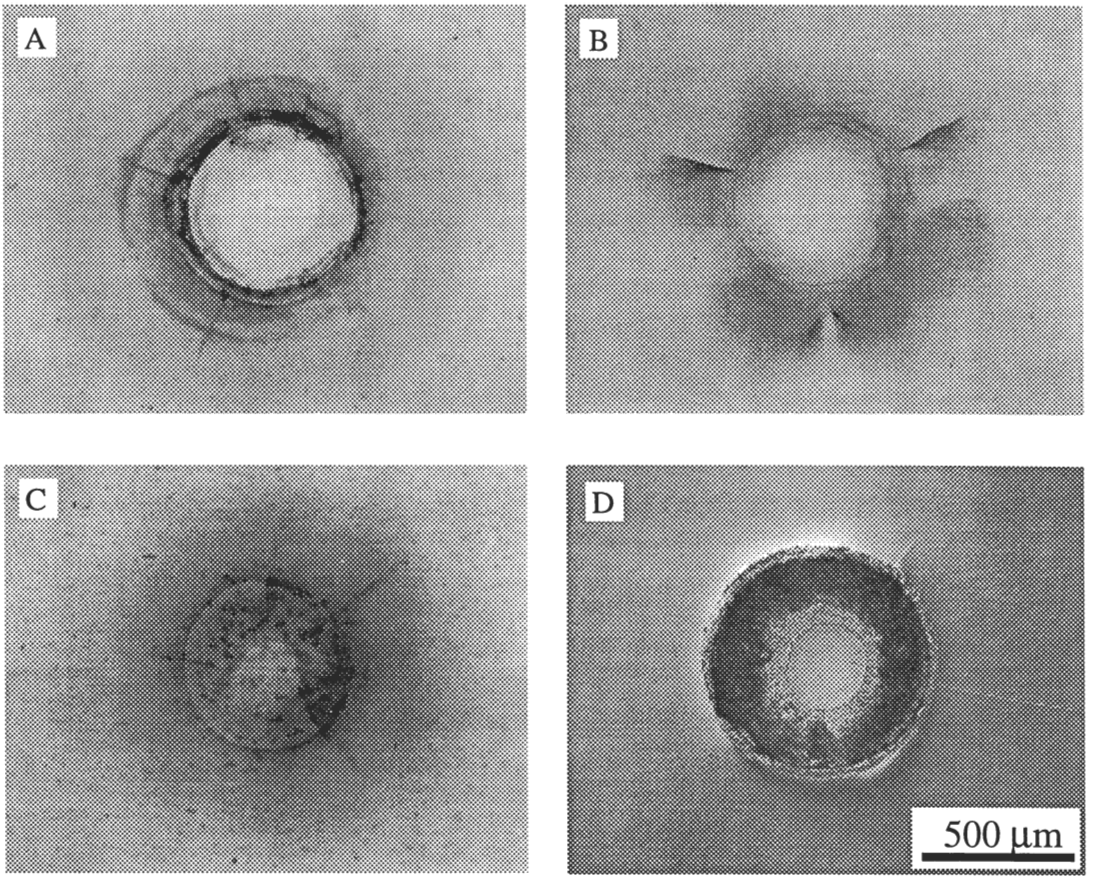

Fig. 6 Surface views of contact damage in (A) porcelain, P = 500 N, $n = 5x10^3$; (B) micaceous glass-ceramic, P = 500 N, $n = 5x10^4$, (C) glass-infiltrated alumina, P = 1000 N, $n = 10^5$ and (D) Y-TZP, P = 3000 N, $n = 10^5$. Indentation with WC spheres (r = 3.18 mm). Note appearance of radially directed cracks at crack periphery. Specimens A, B and C thinned from back surface and viewed in transmitted light. Specimen D viewed in reflected light.

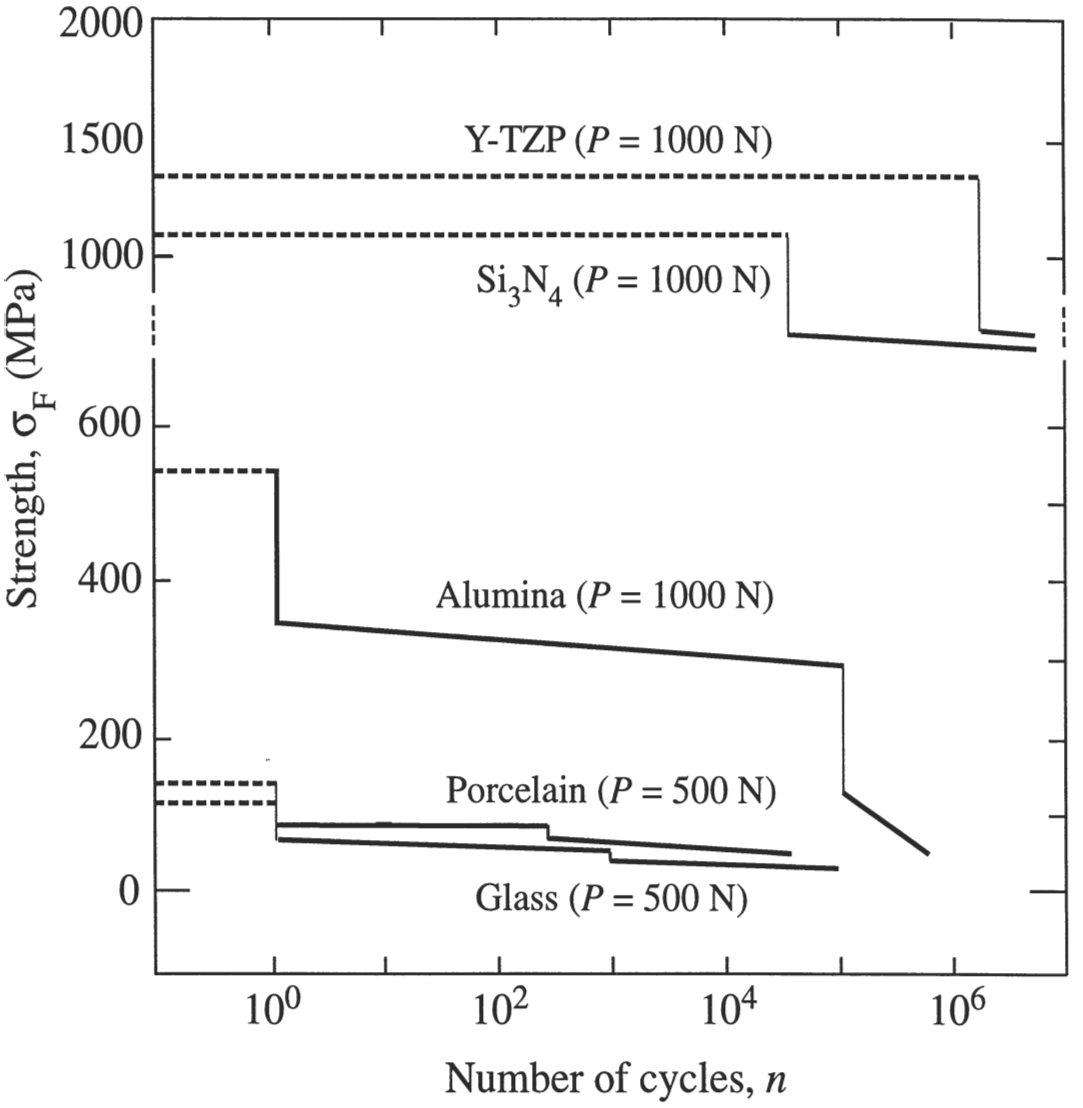

Fig. 7 Master diagram comparing contact fatigue responses for selected materials, at specified contact load P. (Note break in strength axis.)